Title: Prey, not temperature, is the dominant driver of juvenile growth in North Sea sandeels

Running page head: sandeel size declines

Agnes B. Olin[1,2*†], Neil S. Banas[1], Michael R. Heath[1], Peter J. Wright[3], Alan MacDonald[4], Sarah Wanless[5], Francis Daunt[5], John R. Speakman[6,7,8,9], Ruedi G. Nager[2]

[1]Department of Mathematics and Statistics, University of Strathclyde, Glasgow G1 1XH, UK.

[2]School of Biodiversity, One Health and Veterinary Medicine, University of Glasgow, Glasgow G12 8QQ, UK.

[3]Marine Scotland Science, Aberdeen AB11 9DB, UK.

[4]Scottish Association for Marine Science, Oban PA37 1QA, UK.

[5]UK Centre for Ecology & Hydrology, Penicuik EH26 0QB, UK.

[6]School of Biological Sciences, University of Aberdeen, Aberdeen AB24 2TZ, UK

[7]Shenzhen key laboratory of metabolic health, Center for Energy metabolism and Reproduction, Shenzhen Institute of Advanced Technology, Chinese Academy of Sciences, and Shenzhen University of Advanced Technology, Shenzhen, Guangdong province 1068, China.

[8]Institute of Genetics and Developmental Biology, Chinese Academy of Sciences, Beijing 100101, China.

[9]Institute of Health Sciences, China Medical University, Shenyang 110052, China.

*Corresponding author: agnes.olin@slu.se

[†]Present address: Department of Aquatic Resources, Swedish University of Agricultural Sciences, 756 51 Uppsala, Sweden.

ABSTRACT: Declining body sizes are prevalent in marine fish and have been suggested to be a response to increasing temperatures. However, the evidence is mixed and the underlying causes often unknown. Here, we explore drivers of spatio-temporal patterns in size in juvenile lesser sandeel (*Ammodytes marinus*), focusing on ongoing size declines in parts of the North Sea. We combine experimental and field data with theory to develop a biologically realistic dynamic energy budget model that explicitly models feeding, metabolism and energy allocation to produce daily predictions of sandeel length during the growth season from 1979 to 2016 in four North Sea sub-populations. When forced with daily temperature estimates and zooplankton data from the Continuous Plankton Recorder, model predictions largely match observed spatio-temporal patterns. Our results suggest that the most plausible driver of observed size declines in the western North Sea is declining prey densities. In contrast, the direct effect of temperature on sandeel size is small, but interacts with local prey availability so that increasing temperatures may boost growth rates in areas with high food availability but reduce growth rates in areas with low food availability. Our results thus suggest that to understand effects of climate change on fish size we need to account for both direct physiological effects and changes in resource availability. Finally, we show that early-life phenology and turbidity (via its impact on intake rates in the visually foraging sandeel) may also impact sandeel size, highlighting the importance of broadening our view of potential drivers of size declines.

KEY WORDS: global warming; bioenergetic model; sand lance; North Atlantic; shrinking; forage fish

1. INTRODUCTION

Declining body sizes have been proposed as a third "universal response" to climate change, in addition to poleward shifts in distribution and shifts in the timing of seasonal events (Daufresne et al. 2009, Gardner et al. 2011, Sheridan & Bickford 2011). However, the evidence to support this claim is mixed, where body sizes have been shown to both increase and decrease in response to warming (Teplitsky & Millien 2014, Audzijonyte et al. 2020) and trends towards increasing body sizes are equally common in most taxa (Martins et al. 2023). In contrast with other taxa, many populations of marine fish do, however, show evidence of declining average body sizes (Martins et al. 2023). The drivers of these declines and how temperature increases may, or may not, affect fish body size is hotly debated. Several mechanisms have been invoked, such as faster development rates but smaller adult sizes (temperature-size rule), and increasing metabolic rates leaving less resources for growth at all ages (Gardner et al. 2011, Sheridan & Bickford 2011, Cheung et al. 2013, Ikpewe et al. 2021). Several other drivers, including declines in the abundance and quality of food (Korman et al. 2021, Menu et al. 2023, Queiros et al. 2024), size-selective predation and fishing (Swain et al. 2007, Ohlberger et al. 2019), and increased competition (Ohlberger et al. 2023) have also been proposed as key contributors to the size declines. In many cases, the drivers are not yet fully understood. However, teasing apart the underlying mechanisms is important, as size is strongly linked to survival (Levangie et al. 2022) and fecundity (Barneche et al. 2018) and thus affects both abundance and the quality of individual fish, with implications for both sustainable fisheries management (Audzijonyte et al. 2013, Persson et al. 2014) and the growth, survival and reproduction of the piscivorous predators that feed on the fish (e.g. Österblom et al. 2001, Engelhard et al. 2014).

68 One species of fish that has exhibited pronounced declines in size is the lesser sandeel (*Ammodytes*
69 *marinus*), a small lipid-rich shoaling fish inhabiting sandy banks in the north-east Atlantic. It is an
70 important trophic link between the zooplankton and several species of seabirds, marine mammals
71 and piscivorous fish, as well as the target of a substantial fishery (Engelhard et al. 2014). The
72 sandeel shows marked spatio-temporal variation in size-at-age in the North Sea region, with larger
73 body sizes in the north-east, and smaller and declining sizes in the western North Sea (Bergstad et
74 al. 2002, Harris & Wanless 2011, van Deurs et al. 2014, Rindorf et al. 2016, Clausen et al. 2017,
75 Wanless et al. 2018). The size declines in the western North Sea have been observed both in mature
76 adults and in juveniles. Off the coast of southeast Scotland, declining juvenile body sizes from the
77 mid-1970s to 2015 resulted in a 70% decline in energy content (Wanless et al. 2018).
78
79 The drivers behind the sandeel size declines are still unclear. Water temperatures, which are
80 increasing rapidly in the north-east Atlantic (Kessler et al. 2022), have been linked to body size in
81 both lesser sandeels and other *Ammodytes* species (Robards et al. 2002, Eliasen 2013, Rindorf et
82 al. 2016). However, the direction of the relationship is inconsistent and modelling work suggests
83 that temperature is not a strong driver of lesser sandeel growth (MacDonald et al. 2018). Variability
84 in prey availability and composition has long been proposed as the main driver of spatial patterns
85 in sandeel size (Macer 1966, Bergstad et al. 2002, Boulcott et al. 2007), with modelling work
86 suggesting that food availability is a key driver of lesser sandeel growth (MacDonald et al. 2018).
87 Prey availability has declined steeply in several of the locations where sandeel size has declined
88 (Olin et al. 2022), which could have contributed to the observed temporal trends. A shift towards
89 a later start to the growth season of juvenile sandeels has also been proposed as a potential driver
90 of the size declines (Frederiksen et al. 2011), possibly driven by temperature-driven delays in

spawning (Wright et al. 2017) and a mismatch between sandeel phenology and peak availability of larval food (Régnier et al. 2019, 2024). Finally, turbidity has increased within the sandeel's range due to coastal erosion, intensified winds and waves resuspending more sediment, and bottom trawlers stirring up sediment and destroying beds of water-filtering bivalves (Capuzzo et al. 2015, Wilson & Heath 2019). As light conditions have been identified as a key driver of intake rates in the visually foraging sandeel (Winslade 1974b, van Deurs et al. 2015), this may therefore have contributed to the observed size declines. In contrast, neither competition (Rindorf et al. 2016, Henriksen et al. 2021) nor predation (Rindorf et al. 2016) or fishing (Bergstad et al. 2002, Wanless et al. 2004, Rindorf et al. 2016) appear strongly linked to lesser sandeel size.

This study aims to provide insight into causes of the changing growth rates of juvenile sandeel, improving our understanding of drivers of size declines in fish in marine ecosystems under anthropogenic change. To do so, we use a dynamic energy budget model to explore drivers of growth in juvenile lesser sandeels in their first summer. Dynamic energy budget models track energy gains and losses as a function of environmental conditions (e.g. temperature, food) and then translate this into changes in body size and energy reserves (Kooijman 2000, Lika & Nisbet 2000). Such mechanistic models are helpful for teasing apart the roles played by different drivers, enabling us to gain a better insight into the impact of ongoing environmental change on fish body sizes. The model builds on a dynamic energy budget model developed by MacDonald et al. (2018). However, the MacDonald model was parameterised specifically for the north-western North Sea over a short time scale, requiring us to make adjustments in order to allow us to study the large-scale, long-term patterns we were interested in here. This involved breaking processes into tractable sub-processes that could be parameterised using data from experiments and

measurements from the field, providing us with a biologically realistic model that can be more readily extended across space and time. We validate model predictions against field data and then use the model to explore to what degree observed spatio-temporal variation in juvenile sandeel size in the North Sea can be explained by the candidate drivers introduced above — (i) sea surface temperatures, (ii) food availability and composition, (iii) sandeel phenology and (iv) turbidity.

2. MATERIALS AND METHODS

2.1. Dynamic energy budget model

Here, we develop a dynamic energy budget model that covers the first growth season, from metamorphosis to winter dormancy, when the sandeels cease feeding and bury into the sand (MacDonald 2017, van Deurs et al. 2011b). As only a small proportion of sandeels spawn in their first year (<5 % in most areas; Boulcott et al. 2007), reproduction is not included in the model.

The model is constructed around two state variables: reserve energy R (kJ, remobilisable tissue, mostly fat) and structural energy S (kJ, non-remobilisable tissue, such as skeletal tissue). The basic structure involves the allocation of net energy gain (assimilated energy A [kJ day^{-1}], minus metabolic costs M [kJ day^{-1}]) to reserve energy and structural energy (see Figure 1). Assimilated energy is the energy from ingested food, after accounting for assimilation efficiency. The model assumes that metabolic costs are subtracted from assimilated energy and that if the assimilated energy is not enough to meet metabolic costs, the rest is subtracted from reserves. If the assimilated energy is larger than the metabolic cost, a certain proportion f_S of this net energy gain is allocated to structural energy and the rest $(1 - f_S)$ to reserve energy. Reserve energy R (kJ) thus changes as follows:

$$\frac{dR}{dt} = A - M - \frac{dS}{dt} \quad (1)$$

136

137 Structural energy S (kJ) then follows:

$$\frac{dS}{dt} = f_S[A - M]^+ \quad (2)$$

138

139 where $[A - M]^+$ signifies that allocation to structural energy only occurs if net energy gain is
140 positive. The equations are discretised assuming time steps of one day, thus providing daily
141 estimates of reserve and structural energy. To be able to compare the model output to field
142 observations, we translated reserve and structural energy into length and wet weight (see SI1).

143

144 The model is run from metamorphosis (generally mid-May, day 141, see "Initial conditions") until
145 early August (day 212), which is roughly when the growth season ends and the sandeels bury into
146 the sand for winter (van Deurs et al. 2011b, MacDonald 2017). Most of the predictions thus
147 represent length at overwintering, unless predictions are made for an earlier day in order for it to
148 be comparable to observed lengths in field data collected on a specific day (see 2.5). Each model
149 component (ingestion, metabolism, energy allocation) is described briefly in the following
150 subsections, with details provided in the SI (see also Olin 2020). Model parameters are presented
151 in SI2 with descriptions of how the values were derived and an analysis of how sensitive model
152 predictions are to choices of parameter values. All model parameters were derived from the
153 literature or available data, apart from three parameters relating to ingestion which were tuned
154 manually (see SI2 and 2.1.1). The model is implemented in the C programming language, based

155 on an adaptation of the growth component of the model presented in MacDonald et al. (2018). R
156 3.5.2 (R Core Team 2018) was used for data processing and visualisation.
157

158 2.1.1. Assimilated energy

159 Prey availability and composition appear to be a major determinant of growth rates in lesser
160 sandeels (van Deurs et al. 2014, 2015, MacDonald et al. 2018), and several studies indicate that
161 sandeels feed selectively (Godiksen et al. 2006, Christensen 2010, Eliasen 2013). Therefore,
162 particular attention was paid to modelling ingestion (see SI3 for details). This is where the main
163 modifications to the MacDonald model were made, where sub-processes were isolated and
164 modelled explicitly (see Olin 2020 for a detailed comparison of the models). Ingestion is modelled
165 on an hourly basis, assuming a daily feeding window covering the hours of light (Freeman et al.
166 2004, Johnsen et al. 2017), minus one hour for school aggregation in the morning and one hour
167 for school disintegration before the sandeels bury into the sediment for the night (see van Deurs et
168 al. 2011a). Total assimilated energy per day A is then obtained by adding up the ingested energy
169 for each hour of feeding, and multiplying it by the assimilation efficiency (proportion of energy
170 remaining after faecal losses and nitrogenous excretion; Jobling 1993). Based on observations of
171 other *Ammodytes* species, assimilation efficiency is assumed to increase linearly with temperature
172 (Larimer 1992, Gilman 1994; SI3.1). Based on experimental observations, it is also assumed that
173 the sandeels do not feed if there is not enough food to account for the metabolic costs of feeding
174 (Winslade 1974a, van Deurs et al. 2011a). Total assimilated energy A (kJ day^{-1}) is thus calculated
175 as:

$$A = \begin{cases} \epsilon \sum_{h=1}^{h_{active}} i_h, & \epsilon \sum_{h=1}^{h_{active}} i_h - (M_{feed} + M_{SDA}) > 0 \\ 0, & \epsilon \sum_{h=1}^{h_{active}} i_h - (M_{feed} + M_{SDA}) \leq 0 \end{cases} \quad (3)$$

where ϵ is the assimilation efficiency, h_{active} the number of hours feeding, i_h the energy ingested during a given hour, and M_{feed} and M_{SDA} the cost of feeding and synthesising tissue, respectively (see below).

Hourly ingested energy i_h is limited by the available prey as well as gut capacity. To incorporate this, we first modelled the maximum potential intake rate i_{max} (kJ h^{-1}; SI3.2) in response to the prey field, and then, if necessary, down-adjusted this according to remaining gut space (SI3.10). Gut content was therefore also modelled on an hourly basis, based on ingestion and digestion, the latter depending on both temperature and prey energy density (SI3.9). The response to the prey field was modelled as a Holling type II functional response (Holling 1959) into which we incorporated three forms of prey selectivity (Eggers 1977): (1) a prey size-, sandeel length- and light-dependent prey detection distance (SI3.4; this built on a sandeel foraging model by van Deurs et al. 2015), (2) a prey size-dependent capture probability (SI3.6) and (3) active switching (assuming switching behaviour is based on the profitability of each prey search class; see Visser & Fiksen 2013; SI3.2). All these forms of selectivity are supported by observations of sandeels (e.g. Godiksen et al. 2006, Christensen 2010, see Olin 2020 for details). As there were no data to inform the two parameter values that govern capture success, these were tuned to align with observed ratios between size of ingested prey and size of available prey, based on data from Godiksen et al. (2006). For handling time, the third parameter that was manually tuned, we tuned it so that the mean predicted and observed lengths for the years of overlapping data were equal in

197 a time series of measured lengths. See SI2 for details on how the tuning was carried out, and 2.5
198 for more details on the time series of lengths used.

199 2.1.2. Metabolism

200 The model includes three types of metabolic costs: (i) standard metabolic rate (SMR), which is the
201 energy required to cover basic maintenance, (ii) costs associated with feeding behaviour and (iii)
202 costs of synthesising tissue (specific dynamic action, SDA). Total metabolic costs M (kJ day^{-1}) are
203 calculated as:

$$M = \underbrace{\alpha_{met} W^{\beta_{met}} Q_{10}^{T/10}}_{SMR} + \underbrace{FWh_{day}}_{feeding} + \underbrace{\zeta_{SDA} A/\epsilon}_{SDA} \quad (4)$$

204

205 where α_{met} is the SMR coefficient, W is sandeel wet weight (g), β_{met} is the weight-scaling
206 exponent of SMR, T is temperature (°C), Q_{10} describes how the SMR increases with temperature,
207 F is the foraging cost per hour per gram of sandeel, h_{day} is the total number of hours spent out of
208 the sand each day (thus assuming that the cost of school aggregation and disintegration is the same
209 as the cost of foraging), ζ_{SDA} is the SDA coefficient, A is the assimilated energy per day (kJ day^{-1})
210 and ϵ the assimilation efficiency. It is thus assumed that SMR is a function of sandeel weight and
211 temperature, the main predictors of SMR in fish (Clarke & Johnston 1999), that feeding costs are
212 a function of activity and sandeel length, and that SDA is a function of the amount of ingested
213 energy (see SI4 for details).

214 2.1.3. Energy allocation

215 Each day, if the net assimilated energy ($A - M$) is positive, a proportion f_S of this is allocated to
216 structural energy (Eq. 2), and the rest to reserves (Eq. 1). Based on observations in *A. marinus*

(Hislop et al. 1991) and other *Ammodytes* species (Sekiguchi et al. 1976, Robards et al. 1999, Danielsen et al. 2016), we assumed that allocation to structural energy decreases as the length of the sandeel increases (see SI5). Further, as the lipid content of *A. marinus* increases rapidly after a winter of fasting (Hislop et al. 1991, Rindorf et al. 2016), we assumed that allocating energy to reserves is prioritised when reserves are below a certain threshold (see SI5).

2.2. Locations

We ran the model in four locations (Figure 2): Dogger Bank (54.7°N 1.5°E), Firth of Forth (56.3°N 2°W), the East Central Grounds (hereafter: ECG; 57.6°N 4°E) and Shetland (59.8°N 1.3°W). The locations were chosen to represent a range of growth conditions, where the ECG is expected to show the fastest growth and Firth of Forth the slowest (Bergstad et al. 2002, Boulcott et al. 2007), and size declines have been reported in all locations (Harris & Wanless 2011, van Deurs et al. 2014, Clausen et al. 2017, Wanless et al. 2018). The locations represent different sub-populations and separate fisheries management areas, based on evidence from tagging, otolith microchemistry, larval drift modelling and genetic studies (ICES 2024).

2.3. Environmental drivers

The model requires the following environmental drivers: abundances, energy content, image area and length of each prey type, sea surface temperatures, day length, average surface solar irradiance and the diffuse attenuation coefficient a_d, which depends on turbidity.

Daily prey abundances were based on data collected by the Continuous Plankton Recorder (see Olin et al. 2022 for methods; dataset available at doi.org/10.17031/1673). Based on prey found in

239 sandeel stomachs, the prey taxa included copepods, Euphausiacea, Hyperiidea, Decapoda larvae,
240 Appendicularia, fish eggs, fish larvae, *Evadne* spp. and *Podon* spp. A full list of prey taxa with
241 energy content, prey image area, length and search class can be found in Table S2. The prey fields
242 were based on data aggregated over a 135 km radius circle centred on each study location (see
243 Olin et al. 2022; Figure 2). The chosen size of the area results from a trade-off between sample
244 size and the homogeneity of the area it represents. The size of the area, and the between-sample
245 variability in the alignment of zooplankton patches and the Continuous Plankton Recorder
246 transects, means that the prey field input is not an exact representation of available prey in the
247 study location for that year. Therefore, we would not necessarily expect the model to reproduce
248 observed sandeel lengths in a given year, even if the model would correctly capture all relevant
249 mechanisms. Instead, the model should be judged by its ability to capture long-term and large-
250 scale spatio-temporal patterns.
251
252 We obtained temperature estimates from the ERA5 Climate Reanalysis, providing hourly sea
253 surface temperature with a 31×31 km resolution (Copernicus Climate Change Service C3S 2017),
254 averaged to daily values. As sandeels may forage throughout the water column and reside in
255 hydrographically dynamic areas (Tien et al. 2017), it was assumed that surface temperatures were
256 representative for the experienced temperatures at all depths. Hours of daylight were obtained
257 using the function "daylength" in the R-package "geosphere" (Hijmans 2017). Average daily
258 surface irradiance (SI3.5) was calculated using a Fortran subroutine (see Ljungström et al. 2020).
259 The diffuse attenuation coefficient a_d was obtained from observations in hydrodynamic regions
260 corresponding to sandeel habitat (see supplementary materials in Capuzzo et al. 2018) and was
261 assumed to be constant.

2.4. Initial conditions

The initial conditions of the model include length at metamorphosis and day of year at metamorphosis. We used day 141 (21 May in a regular year) as the default starting date and 4 cm as the default starting length, chosen to be broadly representative for the study locations (Wright & Bailey 1996, Jensen 2000, Régnier et al. 2017).

2.5. Model validation

The model was run in all four locations for the years 1979–2016, excluding location-years in which insufficient zooplankton data (fewer than three samples per month) were available (Dogger Bank N = 33, Firth of Forth N = 23, ECG N = 23, Shetland N = 36). We then assessed whether the model could recreate observed large-scale and long-term spatio-temporal patterns in sandeel length, making use of all juvenile length observations we could locate from our study locations. This included (i) fisheries data from Shetland and the ECG collected in 1979 (Bergstad et al. 2002), (ii) dredge surveys in the Firth of Forth, Dogger Bank and a location slightly south of the ECG in 1999 (Boulcott et al. 2007), (iii) dredge surveys since 2006 in the ECG and since 2004 in Dogger Bank (ICES 2024), (iv) sandeels brought in by Atlantic puffins (*Fratercula arctica*) to the Isle of May in the Firth of Forth (Wanless et al. 2018) and (v) corresponding datasets of sandeels collected from puffins in the Shetland area, one from Fair Isle, south of Shetland, and one from Hermaness, in the north of Shetland (Harris & Wanless 2011). The first three datasets are representative of length at overwintering, while the latter two are standardised to the 1st of July. The puffin dataset from the Firth of Forth was used to tune handling time to achieve the same mean length in the predictions as in the observations (see 2.1.1 and SI2), as this is our longest time series and as the area is well-sampled in terms of CPR data. Note that tuning handling time to this time series does

not affect the predicted temporal trend or predicted relative differences in sandeel length between locations, only the absolute length. For this reason, the Firth of Forth dataset is only used to assess whether our predictions reproduce spatio-temporal trends, not whether the absolute values match. For the other locations, absolute values for predictions and observations can be compared since these datasets were not used for tuning, although as described above, we do not expect a match on an annual basis due to the uncertainty in the CPR data. Temporal trends in predictions and observations were assessed using linear regression.

2.6. Drivers of growth

The sensitivity of length predictions to our hypothesised drivers (temperature, food, phenology, light) was then investigated, quantified as the percentage difference in length at overwintering compared to a baseline scenario. To do this, the model was run for all location-years with data, varying one driver at a time while keeping the remaining input at their original values. This approach isolates the effect of individual drivers while also ensuring that the full range of environmental conditions are captured.

To examine the impact of temperature, a baseline annual cycle was established for each location by averaging the sea surface temperature for each day of the year across years. A range of temperature conditions were then examined by adjusting this baseline, from subtracting 3°C (corresponding to coldest year in dataset) to adding 4.5°C (similar to the temperature anomaly of the 2023 heatwave, Berthou et al. 2023). We also compared the average temperature over the growth season for a given year with (i) predicted lengths at overwintering, to assess the relative importance of temperature in driving model predictions, and (ii) actual observed lengths, to determine whether similar patterns are present in field data. As a humped relationship emerged

306 when varying temperature across our defined range (see Results), this was done using both a simple
307 linear regression and a second-order polynomial. To account for any temporal autocorrelation, the
308 models were fitted with a first order auto-regressive error structure. The models were compared
309 using ΔAIC_C.

310 To investigate the role of food, we focused on three aspects: the total amount of available energy,
311 the density of *Calanus finmarchicus* (often identified as a key driver of bottom-up dynamics in
312 this region; Frederiksen et al. 2013, van Deurs et al. 2014) and the prey size, where the availability
313 of large prey is thought to boost sandeel ingestion and growth rates (van Deurs et al. 2015,
314 MacDonald et al. 2018). First, for each location, we varied the total amount of energy available
315 throughout the whole season from the lowest to the highest observed value in the time series by
316 applying a year-specific scalar to daily zooplankton densities in each year with available
317 zooplankton data, thus maintaining seasonal patterns and keeping the relative density of each taxa
318 constant within each year, but standardising the amount of energy across years. Predictions were
319 then averaged across years for each location, at each level of available energy, to obtain the
320 location-specific relationship between available energy and predicted length. Then, we repeated
321 this approach but instead varied only the density of *C. finmarchicus*, from the lowest to the highest
322 mean density observed in each location, keeping all other prey types at their original densities.
323 Again, the seasonal pattern was preserved. For the prey size we took a different approach,
324 exploring the effect of keeping the total available energy for a given day unchanged, but having
325 all energy in just one prey type. The prey types we explored included *Oithona* spp. (0.68 mm),
326 *Acartia* spp. (1.15 mm) and *C. finmarchicus* (2.7 mm), considered representative of small, medium
327 and large prey, respectively. As for temperature, we compared the daily energy availability,
328 average daily *C. finmarchicus* densities and average prey size over the growth season for a given

329 year with (i) predicted lengths at overwintering and (ii) actual observed lengths. This was done
330 using both a simple linear regression and a $\log_{10}$-transformation, as the positive effects were
331 expected to level out. Again, the models were fitted with a first order auto-regressive error structure
332 and were compared using ΔAIC_C. For (ii), we note again that the representativeness of prey field
333 data may vary between years, so results should be interpreted with caution.

334 To assess the impact of phenology and larval growth processes on predicted length, the impact of
335 date of metamorphosis and length at metamorphosis was examined. The day of the year on which
336 the model runs were initiated (equivalent to the metamorphosis date) was varied from 121 to 181,
337 and the initial length (equivalent to the metamorphosis length) was varied from 3.5 to 5.5 cm based
338 on observed ranges (Wright & Bailey 1996, Jensen 2000, Régnier et al. 2017, 2024). As the prey
339 field input was kept constant, varying the model start date is equivalent to examining the role of
340 variation in sandeel phenology relative to prey phenology.

341 Finally, to examine the impact of light conditions, the diffuse attenuation coefficient a_d was varied
342 over the range 0 (completely clear waters) to 0.3, based on a range of values commonly observed
343 in the type of hydrodynamic region corresponding to sandeel habitat (see supplementary materials
344 in Capuzzo et al. 2018).

345 ## 3. RESULTS

346 ### 3.1. Model validation

347 While tuned only to length data from the Firth of Forth, the model also produced realistic
348 predictions for the other locations and reproduced spatial differences in length (Figure 3). Both
349 observations and predictions suggest that (i) in the late 1970s, growth conditions in the ECG were

350 better than in Shetland, (ii) in the late 1990s, growth conditions were better in the ECG than in
351 Dogger Bank, which in turn were better than in the Firth of Forth, and (iii) the better growth
352 conditions in the ECG compared to the Dogger Bank were maintained in the 2000s and 2010s
353 (Figure 3a–d).
354
355 The model predictions also did well in reproducing the temporal trend in the Firth of Forth (Figure
356 3e). Observations showed a decline in sandeel length between 1982 and 2015 of -0.06 [95 % CI: -
357 0.08; -0.04] cm per year. Predictions over the same time period also showed some evidence of a
358 decline, and although a weaker decline of -0.03 [95 % CI: -0.07; 0] cm per year, the 95 %
359 confidence intervals of the two slopes overlapped. In Shetland, predictions pointed to an increase
360 in length by 0.05 [95 % CI: 0.02; 0.09] cm per year (Figure 3f) over the time period 1979–2009
361 (the years for which we had both predictions and observations). This does not align with the
362 observations from Fair Isle, which instead showed a decline of -0.12 [95 % CI: -0.19; -0.06] cm
363 per year, or from Hermaness, where no trend was observed [estimate: 0.02; 95 % CI: -0.15; 0.19].
364
365 In Dogger Bank for the period 2004–2016 when both predictions and observations are available,
366 neither observations [estimate: 0; 95 % CI: -0.08; 0.07] nor predictions [estimate: -0.03; 95 % CI:
367 -0.16; 0.09] showed any trend. There was also no trend in predicted length over the time period
368 1988–2011 during which size declines have been reported in older age groups (van Deurs et al.
369 2014) [estimate: 0.02; 95 % CI: -0.02; 0.05]. In the ECG for the period 2006–2016 when
370 predictions and observations are both available, neither observations [estimate: -0.14; 95 % CI: -
371 0.35; 0.07] nor predictions [estimate: 0.01; 95 % CI: -0.43; 0.45] showed any trend.
372

373 ### 3.2. Drivers of growth

374 #### 3.2.1. Temperature

375 Varying the temperature had a minor impact on predicted sandeel length (<1 % compared to
376 baseline, Figure 4a). The effect was nonlinear, with increased temperatures resulting in increased
377 predicted lengths up to an optimum after which predicted lengths instead decreased. The location
378 of the optima in relation to the baseline varied between locations, so that a temperature increase
379 would likely result in a small decline in body length in the Firth of Forth and Dogger Bank (optima
380 just below average temperatures over the study period), whereas increased lengths were predicted
381 for the ECG and Shetland (optima close to maximal warming). There were no relationships
382 between observed growth season temperatures and predicted length at overwintering (Table S3;
383 Figure 4b). However, in Fair Isle, we saw a negative linear relationship between growth season
384 temperatures and actual observed lengths, where length decreased by 1.6 [95 % CI: 0.92; 2.2] cm
385 per 1°C increase (Table S3; Figure 4c).

386 #### 3.2.2. Food

387 Predicted length was sensitive to average daily energy availability, where a shift from mean to
388 maximum values resulted in a predicted increase in length of up to 14 % and a shift from mean to
389 minimum values resulted in a predicted decrease of up to 38 % (Figure 5a). There were positive,
390 log-shaped relationships between observed average daily energy availability in a given year and
391 predicted length in the same year in the ECG and in Shetland (Table S4; Figure 5b). There was a
392 positive, log-shaped relationship between observed average daily energy availability in a given
393 year and observed length in the same year in Dogger Bank (Table S4; Figure 5c).
394

For *Calanus finmarchicus*, there were clear differences between locations in the role it played. In the Firth of Forth and Dogger Bank, shifting densities over the range observed only resulted in a change in predicted length of ca. 1–5 %, whereas in the ECG, a shift from mean to maximum values resulted in a predicted increase of 16 % and a shift from mean to minimum values resulted in a predicted decrease of 10 %, and the corresponding values for Shetland were 16 % and 2 %, respectively (Figure 5d). There were positive, log-shaped relationships between observed *C. finmarchicus* densities and predicted length in the ECG and in Shetland (Table S4; Figure 5e). We saw no relationships between observed *C. finmarchicus* densities and observed length (Table S4; Figure 5f).

Prey type had a large effect on predicted lengths. For all three prey size classes examined, the predicted sandeel lengths increased with total available energy, but at peak energy availability, the predicted length for sandeels was ca. 15 cm when prey was supplied as large *C. finmarchicus*, whereas it was only ca. 6 cm when prey was supplied as small *Oithona* spp. (Figure 5g). There was a positive, linear relationship between observed average prey size during the growth season and predicted length in the ECG, and a negative, linear relationship in the Firth of Forth (Table S4; Figure 5h). In Hermaness, there was a positive, linear relationship between average prey size and observed length (Table S4; Figure 5i).

3.2.3. Timing and length at metamorphosis

The effect of timing of metamorphosis was larger than the effect of length at metamorphosis (Figure 6). For the nominal value of length at metamorphosis (4 cm), a shift to the earliest date examined (day 121) resulted in a predicted increase in length at overwintering of 4–7 %, whereas a shift to the latest date examined (day 181) resulted in a decrease of 10–23 %. For the nominal

418 value of timing of metamorphosis (day 141), a shift to the smallest length examined (3.5 cm)
419 resulted in a predicted decrease in length at overwintering of 1–2 %, whereas a shift to the largest
420 examined (5.5 cm) resulted in an increase of 3–7 %.

421 3.2.4. Light conditions

422 A shift towards increased turbidity (higher values for the diffuse attenuation coefficient a_d)
423 resulted in a decline in predicted sandeel length of up to ca. 50–60 % (Figure 7). A shift to
424 completely clear waters only increased predicted length by ca. 3 %.

425 4. DISCUSSION

426 This study used a dynamic energy budget model to explore plausible drivers of spatio-temporal
427 variation in the growth of juvenile lesser sandeels in the North Sea region, with a particular focus
428 on observed size declines. Model predictions matched observed spatio-temporal patterns well. Our
429 results suggest that the effect of temperature on sandeel growth was minor, but varies in direction
430 over space, and that it is unlikely that direct effects of increasing temperatures explain the size
431 declines. In contrast, our results indicate that composition and density of prey are important drivers
432 of sandeel growth rates. Variation in the timing of metamorphosis, and thus the start of the growth
433 season, may also play a role in driving variation in size. Finally, turbidity could potentially have a
434 large impact on sandeel growth via its effect on prey detectability.
435
436 As the direct effect of temperature was small, and light conditions as well as size at
437 metamorphosis and timing of metamorphosis were kept constant, the model's ability to reproduce
438 the decline in size observed in the Firth of Forth suggests that trends in the composition and
439 abundance of prey were sufficient to explain the observed size decline. This supports the

hypothesis that a change in food conditions may be one of the key mechanisms behind the widespread declines in size observed in many organisms (Gardner et al. 2011), including fish (Korman et al. 2021, Menu et al. 2023). The decline in available food for the sandeels is primarily driven by declining abundances of small copepods (Olin et al. 2022). This explains the negative correlation between prey size and predicted sandeel length in the Firth of Forth (Figure 5h), as the larger average prey sizes result from low densities of small copepods (Olin et al. 2022). Tyldesley et al. (2024) showed that these declines in small copepod densities, and in total energy available to planktivorous fish, are widespread across the northwest European shelf and beyond, extending as far as Iceland and the southern Bay of Biscay. The ultimate driver is not known, but it could be linked to a decline in local primary productivity associated with increasing temperatures and decreased nutrient input (Capuzzo et al. 2018), possibly together with reduced quality and shifting phenology of the phytoplankton (Schmidt et al. 2020). The decline in sandeel size could thus still be related to climate change, via a change in prey availability and composition.

Food conditions are also a plausible driver of the spatial patterns in sandeel size, as long hypothesised (Macer 1966, Bergstad et al. 2002; Boulcott et al. 2007). Densities of *Calanus* spp. are higher in the north (Olin et al. 2022), and correlate with predicted growth in the ECG and Shetland (Figure 5e). Our results further suggest that a prey field composed of large, *Calanus*-like prey provides better growth conditions than smaller prey types, even when the total amount of energy is the same (Figure 5g), corroborating previous work showing the importance of prey size, in both lesser sandeels and other species (van Deurs et al. 2015, MacDonald et al. 2018, Ljungström et al. 2020). It is thus likely that the high densities of *Calanus* spp. explain why the sandeels grow so fast in the ECG. Previously, *C. finmarchicus* dominated the study area, but since

463 the early 2000s, they are increasingly being replaced by *C. helgolandicus* (Olin et al. 2022,
464 Tyldesley et al. 2024). This is likely the result of an ongoing temperature-driven northward
465 distribution shift of both *Calanus* species (Edwards et al. 2020). In the northern North Sea, this
466 shift may have a negative effect on sandeel growth in the long term, as the phenology of *C.*
467 *helgolandicus* is less well matched with the sandeel growth season, and as, at least so far, peak
468 densities of *C. helgolandicus* in the study area do not match those of *C. finmarchicus* (see Edwards
469 et al. 2020, Olin et al. 2022). In comparison, densities of *C. finmarchicus* are, and have been, lower
470 in the western North Sea (which is further away from where *C. finmarchicus* enter the North Sea
471 from the north; Heath et al. 1999), and are not positively correlated with predicted or observed
472 sandeel growth in this area (Figure 5e–f). This may result from the low densities in the area and is
473 in line with recent evidence from Dogger Bank (Henriksen et al. 2018) and the Firth of Forth
474 (Régnier et al. 2017, MacDonald et al. 2018), suggesting that the role of *C. finmarchicus* in driving
475 sandeel dynamics may have been overestimated in these areas in previous studies (see e.g. van
476 Deurs et al. 2009, 2014, Frederiksen et al. 2013).
477
478 The direct effect of temperature on sandeel growth was minor, resulting in a 1% difference
479 in predicted size at most, even at a 4.5°C increase (Figure 4a). Our approach relied on the
480 assumption that sea surface temperatures are indicative of temperatures throughout the water
481 column. How valid this assumption is likely varies over both space and time (see van Leeuwen et
482 al. 2015), which may have affected our predictions slightly, and also the identified relationships
483 between temperature and observed lengths. However, importantly, this does not affect our
484 conclusion that the direct effect of temperature is minor, as this emerges from the mechanisms
485 included in the model, not the data used to run it. Further, it is important to note that not all possible

temperature effects on sandeel feeding and growth have been included in the model. For example, it does not capture a possible effect of temperature on detection distance, which has been seen in other planktivorous fish (Gliwicz et al. 2018), as it is unknown whether this process is present in sandeel. Importantly, the model was designed to reflect the current state of knowledge, and the small direct effect of temperature is in line with results presented by MacDonald et al. (2018), which were also based on a dynamic energy budget model of lesser sandeel, as well as work on other fish species (e.g. Menu et al. 2023). This suggests that temperature-driven increases in metabolic costs, which have been proposed as one of the mechanisms behind climate change-associated body size declines (Sheridan & Bickford 2011), are not the main cause of sandeel size declines.

In our model, warmer temperatures lead to greater assimilation efficiency and faster digestion rates, which allows for higher intake and growth rates. However, warmer temperatures also lead to increased metabolic costs, which result in a negative net energy gain if the increased costs are not outweighed by increased energy assimilation, which may be the case if food conditions are poor. This is why our study locations responded differently to temperature, where warmer temperatures led to higher growth rates in locations where food conditions are good (ECG, Shetland, high densities of *Calanus* spp.), but reduced growth rates where food conditions are poorer (Firth of Forth, Dogger Bank). This means that if a changing climate results in poorer food conditions, declines in growth rates may be mildly exacerbated by the increased metabolic costs of higher temperatures. Régnier et al. (2024) identified a similar pattern in sandeel larvae, where temperature had a positive effect on growth when the match between sandeel hatching and the peak availability of larval food was good, while the effect was instead negative when the match

was poor. This type of interaction has also been noted in other fish species (Brett et al. 1969, Allen & Wootton 1982, Ohlberger 2013). Our study thus supports the claim that to understand effects of climate change on fish, we need to account for both direct physiological effects and changes in resource availability (Huey & Kingsolver 2019, Lindmark et al. 2022).

Our model only covered the first growth season, and therefore we could not fully evaluate the support for the temperature-size rule (i.e. fast development and smaller size-at-maturation, e.g. Gardner et al. 2011, Ikpewe et al. 2021). However, our model did suggest that if food is sufficient, temperature increases do result in boosted juvenile growth, in line with the temperature-size rule. As for size-at-maturation, a study from 1999 showed that Firth of Forth sandeels matured at a smaller size than Dogger Bank sandeels, which in turn matured at a smaller size than ECG sandeels (Boulcott et al. 2007). As the average annual temperature in the Firth of Forth was lower than in the other two locations, this does not fit with a smaller size-at-maturation in warmer temperatures. However, a more recent study found no significant differences in the relationship between size and maturation rates in these locations (Wright et al. 2019), and the difference in average annual temperatures between the locations is small (usually <1°C), so a broader geographical area would likely be needed to evaluate the support for the temperature-size rule in lesser sandeels.

While the potential effect of timing of metamorphosis on sandeel length-at-age was considerable, it cannot explain the size declines in the Firth of Forth on its own: the model predicts that a shift from the earliest to the latest observed date of metamorphosis in the Firth of Forth (Régnier et al. 2017) only results in a length difference of around 12% and thus cannot alone explain the decline in length of 28% over the study period. Further, there is no marked temporal

trend (or spatial pattern) in larval or settlement phenology within the study area (Lynam et al. 2013, Régnier et al. 2019, 2024), and estimates of date at settlement for the Firth of Forth from recent years actually suggest that they are rather in the earlier part of the range we examined (Régnier et al. 2024). This provides further support for deteriorating food conditions as the most plausible driver of observed sandeel size declines in the Firth of Forth. Still, considering that phenology shifts are a common response to climate change in marine ecosystems (Poloczanska et al. 2013), temporal mismatch with prey may be a useful driver to consider in other cases of marine fish size declines.

As for the effect of turbidity, the potential role played was large. The findings here echo those based on studies of visually foraging fish in general (Aksnes 2007, Ljungström et al. 2020, Korman et al. 2021) and of *A. marinus* in particular (van Deurs et al. 2015). Turbidity in the North Sea varies seasonally and over space (e.g. Capuzzo et al. 2013) and has increased over time (Capuzzo et al. 2015, Wilson & Heath 2019). While satellite- and model-based estimates of turbidity are available for the North Sea, they do not extend far enough back in time to be used as input for the model. Still, an interesting avenue for future research would be to explore spatio-temporal patterns in turbidity in sandeel grounds using these datasets. Increasing turbidity may also impair the foraging success of visually foraging sandeel predators (Finney et al. 1999, Lewis et al. 2015, Darby et al. 2022), suggesting that impacts could amplify up the trophic chain.

While the model predictions generally agreed with observations, this was not the case in Shetland. However, while predicted lengths were greater than those of the sandeels collected by puffins, they do match observations from trawl surveys from 1990–1992 (Wright & Bailey 1996;

555 see Figure 4.2 in Olin, 2020) and from 2002–2007 (Marine Scotland Science, unpubl. data), the
556 latter estimating mean juvenile lengths in August to 8–10.5 cm, overlapping with our predictions
557 at overwintering for the same time period (9.6–11.5 cm). As the time series from Fair Isle and
558 Hermaness show different trends, possibly since the Fair Isle puffins may go south to Orkney to
559 forage, it is also difficult to know whether the size of Shetland sandeels have changed over time.
560 Still, there is no empirical data that support the increase in length in the early 2000s predicted by
561 the model, which is driven by an increased availability of food (Olin et al. 2022). Possibly, the
562 benefits of increasing food availability during the juvenile feeding season have been cancelled out
563 by a decline in food availability for fish larvae in the early 2000s (see Alvarez-Fernandez et al.
564 2012). Interestingly, poor breeding success and delayed breeding of sandeel-eating seabirds was
565 also observed in the early 2000s in this region (JNCC 2016, Maniszewska 2019, Olin et al. 2020)
566 suggesting that this time period warrants further study. The negative relationship between observed
567 length and growth season temperatures in Fair Isle may also be worth exploring further.
568
569 In Dogger Bank, the predictions did not show evidence of a decline over the time period
570 during which size declines have been reported in age 1 and age 2 sandeels (1988–2011; van Deurs
571 et al. 2014). However, a closer examination of the published time series suggests that a significant
572 decline only occurred in age 2 sandeel (see Figure S3 in SI6). No data exist on juvenile sandeel
573 from the same time period so it is unclear whether a size decline in juvenile sandeels has actually
574 occurred in Dogger Bank. Over the time period for which we have both observations and
575 predictions, no decline was evident (Figure 3a). Similarly, we observed no clear decline in the
576 predicted or observed size of sandeels in the ECG (Figure 3c), while a shift from larger to smaller
577 sizes was observed in the 1990s in the eastern North Sea (Clausen et al. 2017) based on sandeels

578 from the fishery, which usually catches older age groups. A difference in trends between age
579 groups may imply that additional mechanisms are at play in older, mature sandeels, for example
580 increased investment into reproduction as temperatures increase (see Wootton et al. 2022; but see
581 also Wright et al. 2017).
582
583 The environmental drivers included were chosen to reflect the current state of knowledge of drivers
584 of sandeel size and growth. However, there are additional drivers that may also have contributed
585 to the observed patterns. Increased predator pressure may result in the sandeels spending less time
586 feeding (see van Deurs et al. 2010) or spend more time engaged in costly predator avoidance
587 behaviour (see Pitcher & Wyche 1983), which would both contribute to reduced intake rates and
588 subsequent growth. These mechanisms could act throughout the feeding season, but may also mean
589 that overwintering is initiated earlier (see van Deurs et al. 2010). As sandeel predators are more
590 abundant further north (ICES 2017), this could be another potential contributor to the disparity
591 between observed and predicted length in Shetland. The initiation of overwintering may depend
592 not only on predation risk, but also on the attainment of sufficient resources (MacDonald 2017,
593 van Deurs et al. 2011b). This mechanism may act as a buffer on overwintering lengths, as the
594 sandeels may extend the feeding window (and thus increase their size) if food availability is low.
595 This could mean that our simplifying assumption of a constant overwintering date could have
596 resulted in slightly exaggerated relationships between prey and sandeel size as this buffering
597 mechanism is not accounted for.
598
599 In summary, our results suggest that if we continue on the current trajectory of increasing
600 temperatures (Kessler et al. 2022) prompting delays in phenology (see Wright et al. 2017, Régnier

et al. 2019), increasing turbidity (Capuzzo et al. 2015, Wilson & Heath 2019), as well as shifts from *C. finmarchicus* to *C. helgolandicus* in the northernmost areas and declining densities of small copepods in the southernmost areas (Edwards et al. 2020), sandeel sizes may decline further. Our results suggest that sandeel growth conditions have deteriorated in the western North Sea, and as smaller sandeels have higher mortality rates, lower maturation rates and lower fecundity (Boulcott et al. 2007, Boulcott & Wright 2011, MacDonald et al. 2018) this may make the sandeel stock vulnerable to additional mortality from fishing. While one could expect that reduced densities as a result of fishing could contribute to increased growth rates via reduced competition, earlier studies of North Sea sandeels do not support any negative relationship between density and growth (Bergstad et al. 2002, Eliasen 2013; Rindorf et al. 2016, Henriksen et al. 2021). As such, a precautionary approach to fishing that takes the changing growth conditions into account may be become increasingly important.

The study provides some lessons of general interest. First, it lends support to the idea of temperature not as a driver that directly and uniformly pushes fish towards smaller body sizes, but rather a driver with complex direct and indirect effects, which may ultimately also result in increases in size in some contexts (see also Audzijonyte et al. 2020). Second, it highlights the importance of considering the prey field from the point of view of the predator, with a local perspective. It is tempting to identify key metrics such as, for example, the abundance of key prey taxa or average size of the prey to try to explain variation in growth. However, due to complex interactions depending on both prey and predator size and acting via, for example, capture success and switching mechanisms, the relationship between these metrics and predator growth may not always play out in a linear fashion, and may break down when extrapolating across space. For

example, variation in *C. finmarchicus* densities is a good predictor of growth in the northern North Sea, but not in the western North Sea. Resolving these foraging dynamics may thus improve our understanding of how oceanographic change travels up the food chain all the way to top predators. Finally, the results also highlight the importance of broadening our view when it comes to identifying drivers of size declines. Our oceans are not only becoming warmer, but there are also trends, in various directions, in top predator densities, nutrient levels and fishing pressure, just to mention a few examples. A broader view of potential drivers helps to better partition variation between different mechanisms, ultimately improving our understanding of how marine ecosystems are responding to an increasingly changing environment.

Acknowledgements

We want to thank Anna Rindorf, Dougie Speirs, Mikael van Deurs, Quentin Quieros, Max Lindmark and three anonymous reviewers for constructive and valuable input. We are also grateful to Espen Johnsen and Mikael van Deurs for providing sandeel data. A.B.O. was funded by a doctoral fellowship from the Marine Alliance for Science and Technology Scotland (MASTS), in partnership with the University of Strathclyde and the University of Glasgow. The present work was part of A.B.O.'s PhD thesis and is also available as a preprint at doi.org/10.1101/2025.03.25.643521. N.S.B. was supported by the UK Missing Salmon Alliance under the Likely Suspects Framework project and the Natural Environment Research Council (Grant Number NE/X008983/1). R.G.N. was supported by the Natural Environment Research Council and the Department for Environment, Food, and Rural Affairs (Grant Number NE/L003090/1). We thank Mike Harris, Mark Newell and all members of the Isle of May field teams for the collection of puffin prey data. The Isle of May study was funded by NERC Award number NE/R016429/1 as part of the UK-SCaPE programme delivering National Capability.

LITERATURE CITED

Aksnes DL (2007) Evidence for visual constraints in large marine fish stocks. Limnol Oceanogr 52:198–203.

Allen JRM, Wootton RJ (1982) The effect of ration and temperature on the growth of the three-spined stickleback, *Gasterosteus aculeatus* L. J Fish Biol 20:409–422.

Alvarez-Fernandez S, Lindeboom H, Meesters E (2012) Temporal changes in plankton of the North Sea: community shifts and environmental drivers. Mar Ecol Prog Ser 462:21–38.

Audzijonyte A, Kuparinen A, Gorton R, Fulton EA (2013) Ecological consequences of body size decline in harvested fish species: positive feedback loops in trophic interactions amplify human impact. Biol Lett 9:20121103.

Audzijonyte A, Richards SA, Stuart-Smith RD, Pecl G, Edgar GJ, Barrett NS, Payne N, Blanchard JL (2020) Fish body sizes change with temperature but not all species shrink with warming. Nat Ecol Evol 4:809–814.

Barneche DR, Robertson DR, White CR, Marshall DJ (2018) Fish reproductive-energy output increases disproportionately with body size. Science 360:642–645.

Bergstad OA, Høines ÅS, Jørgensen T (2002) Growth of sandeel, *Ammodytes marinus*, in the northern North Sea and Norwegian coastal waters. Fish Res 56:9–23.

Berthou S, Renshaw R, Smyth T, Tinker JP, Grist J, Wihsgott JU, Jones S, Inall M, Nolan G, Berx B, Arnold A, Blunn LP, Castillo JM, Cotterill D, Daly E, Dow G, Gómez B, Fraser-Leonhardt V, Hirschi JJ-M, Lewis HW, Mahmood S, Worsford M (2024) Exceptional atmospheric conditions in June 2023 generated a northwest European marine heatwave which contributed to breaking land temperature records. Commun Earth Environ 5:287

670 Boulcott P, Wright PJ, Gibb FM, Jensen H, Gibb IM (2007) Regional variation in maturation of
671 sandeels in the North Sea. ICES J Mar Sci 64:369–376.
672 Boulcott P, Wright PJ (2011) Variation in fecundity in the lesser sandeel: implications for
673 regional management. J Mar Biol Assoc UK 91: 1273–1280.
674 Brett JR, Shelbourn JE, Shoop CT (1969) Growth Rate and Body Composition of Fingerling
675 Sockeye Salmon, *Oncorhynchus nerka*, in relation to Temperature and Ration Size. J Fish
676 Board Can 26:2363–2394.
677 Capuzzo E, Lynam CP, Barry J, Stephens D, Forster RM, Greenwood N, McQuatters-Gollop A,
678 Silva T, van Leeuwen SM, Engelhard GH (2018) A decline in primary production in the
679 North Sea over 25 years, associated with reductions in zooplankton abundance and fish
680 stock recruitment. Glob Change Biol 24:e352–e364.
681 Capuzzo E, Painting SJ, Forster RM, Greenwood N, Stephens DT, Mikkelsen OA (2013)
682 Variability in the sub-surface light climate at ecohydrodynamically distinct sites in the
683 North Sea. Biogeochemistry 113:85–103.
684 Capuzzo E, Stephens D, Silva T, Barry J, Forster RM (2015) Decrease in water clarity of the
685 southern and central North Sea during the 20th century. Glob Change Biol 21:2206–
686 2214.
687 Christensen V (2010) Behavior of Sandeels Feeding on Herring Larvae. Open Fish Sci J 3:164–
688 168.
689 Clarke A, Johnston NM (1999) Scaling of metabolic rate with body mass and temperature in
690 teleost fish. J Anim Ecol 68:893–905.
691 Clausen LW, Rindorf A, van Deurs M, Dickey-Collas M, Hintzen NT (2018) Shifts in North Sea
692 forage fish productivity and potential fisheries yield. J Appl Ecol 55:1092–1101.

693 Copernicus Climate Change Service C3S (2017) ERA5: Fifth generation of ECMWF
694 atmospheric reanalyses of the global climate.
695 Danielsen N, Hedeholm R, Grønkjær P (2016) Seasonal changes in diet and lipid content of
696 northern sand lance *Ammodytes dubius* on Fyllas Bank, West Greenland. Mar Ecol Prog
697 Ser 558:97–113.
698 Darby J, Clairbaux M, Bennison A, Quinn JL, Jessopp MJ (2022) Underwater visibility
699 constrains the foraging behaviour of a diving pelagic seabird. Proc R Soc B Biol Sci
700 289:20220862.
701 Daufresne M, Lengfellner K, Sommer U (2009) Global warming benefits the small in aquatic
702 ecosystems. Proc Natl Acad Sci 106:12788–12793.
703 van Deurs M, Behrens JW, Warnar T, Steffensen JF (2011a) Primary versus secondary drivers of
704 foraging activity in sandeel schools (*Ammodytes tobianus*). Mar Biol 158:1781–1789.
705 van Deurs M, Christensen A, Frisk C, Mosegaard, H (2010) Overwintering strategy of sandeel
706 ecotypes from an energy/predation trade-off perspective. Mar Ecol Prog Ser 416: 201–
707 214.
708 van Deurs M, van Hal R, Tomczak M, Jónasdóttir S, Dolmer P (2009) Recruitment of lesser
709 sandeel *Ammodytes marinus* in relation to density dependence and zooplankton
710 composition. Mar Ecol Prog Ser 381:249–258.
711 van Deurs M, Hartvig M, Steffensen JF (2011b) Critical threshold size for overwintering
712 sandeels (*Ammodytes marinus*). Mar Biol 158:2755–2764.
713 van Deurs M, Jørgensen C, Fiksen Ø (2015) Effects of copepod size on fish growth: a model
714 based on data for North Sea sandeel. Mar Ecol Prog Ser 520:235–243.
715 van Deurs M, Koski M, Rindorf A (2014) Does copepod size determine food consumption of

716 particulate feeding fish? ICES J Mar Sci 71:35–43.
717 Edwards M, Atkinson A, Bresnan E, Helaouet P, McQuatters-Gollop A, Ostle C, Pitois S,
718 Widdicombe C (2020) Plankton, jellyfish and climate in the North-East Atlantic. MCCIP
719 Sci Rev 2020:32 pages.
720 Eggers DM (1977) The nature of prey selection by planktivorous fish. Ecology 58:46–59.
721 Eliasen K (2013) Sandeel, *Ammodytes* spp., as a link between climate and higher trophic levels
722 on the Faroe shelf. PhD, University of Aarhus, Aarhus
723 Engelhard GH, Peck MA, Rindorf A, Smout S, van Deurs M, Raab K, Andersen KH, Garthe S,
724 Lauerburg RAM, Scott F, Brunel T, Aarts G, van Kooten T, Dickey-Collas M (2014)
725 Forage fish, their fisheries, and their predators: who drives whom? ICES J Mar Sci
726 71:90–104.
727 Finney SK, Wanless S, Harris MP (1999) The effect of weather conditions on the feeding
728 behaviour of a diving bird, the Common Guillemot *Uria aalge*. J Avian Biol: *30* 23–30.
729 Frederiksen M, Anker-Nilssen T, Beaugrand G, Wanless S (2013) Climate, copepods and
730 seabirds in the boreal Northeast Atlantic - current state and future outlook. Glob Change
731 Biol 19:364–372.
732 Frederiksen M, Elston D, Edwards M, Mann A, Wanless S (2011) Mechanisms of long-term
733 decline in size of lesser sandeels in the North Sea explored using a growth and phenology
734 model. Mar Ecol Prog Ser 432:137–147.
735 Freeman S, Mackinson S, Flatt R (2004) Diel patterns in the habitat utilisation of sandeels
736 revealed using integrated acoustic surveys. J Exp Mar Biol Ecol 305:141–154.
737 Gardner JL, Peters A, Kearney MR, Joseph L, Heinsohn R (2011) Declining body size: a third
738 universal response to warming? Trends Ecol Evol 26:285–291.

739 Gilman SL (1994) An energy budget for northern sand lance, *Ammodytes dubius*, on Georges
740 Bank, 1977-1986. Fish Bull 92:647–654.
741 Gliwicz ZM, Babkiewicz E, Kumar R, Kunjiappan S, Leniowski K (2018). Warming increases
742 the number of apparent prey in reaction field volume of zooplanktivorous fish. Limnol
743 Oceanogr 63: S30–S43.
744 Godiksen JA, Hallfredsson EH, Pedersen T (2006) Effects of alternative prey on predation
745 intensity from herring *Clupea harengus* and sandeel *Ammodytes marinus* on capelin
746 *Mallotus villosus* larvae in the Barents Sea. J Fish Biol 69:1807–1823.
747 Harris MP, Wanless S (2011) The Puffin. T & AD Poyser, London.
748 Heath MR, Backhaus JO, Richardson K, McKenzie E, Slagstad D, Beare D, Dunn J, Fraser JG,
749 Gallego A., Hainbucher D, Hay S, Jónasdóttir S, Madden H, Mardaljevic J, Schacht A
750 (1999). Climate fluctuations and the spring invasion of the North Sea by *Calanus*
751 *finmarchicus*. Fish Oceanogr 8:163–176.
752 Henriksen O, Christensen A, Jonasdottir S, MacKenzie BR, Nielsen K, Mosegård H, van Deurs
753 M (2018) Oceanographic flow regime and fish recruitment: reversed circulation in the
754 North Sea coincides with unusually strong sandeel recruitment. Mar Ecol Prog Ser
755 607:187–205.
756 Henriksen O, Rindorf A, Brooks ME, Lindegren M, van Deurs M (2021) Temperature and body
757 size affect recruitment and survival of sandeel across the North Sea. ICES J Mar Sci
758 78:1409–1420.
759 Hijmans RJ (2017) Geosphere: Spherical trigonometry.
760 Hislop JRG, Harris MP, Smith JGM (1991) Variation in the calorific value and total energy
761 content of the lesser sandeel (*Ammodytes marinus*) and other fish preyed on by seabird. J

762 Zool 224:501–517.
763 Holling CS (1959) Some characteristics of simple types of predation and parasitism. Can
764 Entomol 91:385–398.
765 Huey RB, Kingsolver JG (2019) Climate Warming, Resource Availability, and the Metabolic
766 Meltdown of Ectotherms. Am Nat 194:E140–E150.
767 ICES. (2017) Report of the Benchmark Workshop on Sandeel (WKSand 2016), 31 October - 4
768 November 2016. Bergen, Norway. ICES CM 2016/ACOM:33.
769 ICES (2024) Benchmark Workshop on Sandeel (*Ammodytes* spp.) (Outputs from 2022 and 2023
770 meetings) (WKSANDEEL). ICES Scientific Reports.
771 Ikpewe IE, Baudron AR, Ponchon A, Fernandes PG (2021) Bigger juveniles and smaller adults:
772 Changes in fish size correlate with warming seas. J Appl Ecol 58:847–856.
773 Jensen H (2000) Settlement dynamics in the lesser sandeel *Ammodytes marinus* in the North Sea.
774 PhD, University of Aberdeen
775 Jensen H, Rindorf A, Wright PJ, Mosegaard H (2011) Inferring the location and scale of mixing
776 between habitat areas of lesser sandeel through information from the fishery. ICES J Mar
777 Sci 68:43–51.
778 JNCC (2016) Seabird population trends and causes of change: 1986-2015 Report.
779 Jobling M (1993) Bioenergetics: feed intake and energy partitioning. In: *Fish ecophysiology*.
780 Rankin JC, Jensen FB (eds) Springer, Dordrecht, p 1–44
781 Johnsen E, Rieucau G, Ona E, Skaret G (2017) Collective structures anchor massive schools of
782 lesser sandeel to the seabed, increasing vulnerability to fishery. Mar Ecol Prog Ser
783 573:229–236.
784 Kessler A, Goris N, Lauvset SK (2022) Observation-based sea surface temperature trends in

785 Atlantic large marine ecosystems. Prog Oceanogr 208:102902.
786 Kooijman SALM (2000) Dynamic energy and mass budgets in biological systems, 2nd ed.
787 Cambridge University Press, Cambridge.
788 Korman J, Yard MD, Dzul MC, Yackulic CB, Dodrill MJ, Deemer BR, Kennedy TA (2021)
789 Changes in prey, turbidity, and competition reduce somatic growth and cause the collapse
790 of a fish population. Ecol Monogr 91:e01427.
791 Larimer S (1992) Aspects of the bioenergetics and ecology of sand lance of Georges Bank. PhD,
792 University of Rhode Island
793 van Leeuwen SP, Tett P, Mills D, van der Molen J (2015) Stratified and nonstratified areas in the
794 North Sea: Long-term variability and biological and policy implications. J Geophys Res
795 Oceans 120:4670–4686.
796 Levangie PEL, Blanchfield PJ, Hutchings JA (2022) The influence of ocean warming on the
797 natural mortality of marine fishes. Environ Biol Fishes 105:1447–1461.
798 Lewis S, Phillips RA, Burthe SJ, Wanless S, Daunt F. (2015) Contrasting responses of male and
799 female foraging effort to year-round wind conditions. J Anim Ecol 84:1490–6.
800 Lika K, Nisbet RM (2000) A Dynamic Energy Budget model based on partitioning of net
801 production. J Math Biol 41:361–386.
802 Lindmark M, Audzijonyte A, Blanchard JL, Gårdmark A (2022) Temperature impacts on fish
803 physiology and resource abundance lead to faster growth but smaller fish sizes and yields
804 under warming. Glob Change Biol 28:6239–6253.
805 Ljungström G, Claireaux M, Fiksen Ø, Jørgensen C (2020) Body size adaptions under climate
806 change: zooplankton community more important than temperature or food abundance in
807 model of a zooplanktivorous fish. Mar Ecol Prog Ser 636:1–18.

Lynam CP, Halliday NC, Höffle H, Wright PJ, Van Damme CJG, Edwards M, Pitois SG (2013) Spatial patterns and trends in abundance of larval sandeels in the North Sea: 1950–2005. ICES J Mar Sci 70:540–553.

MacDonald A (2017) Modelling the impact of environmental change on the physiology and ecology of sandeels. PhD, University of Strathclyde, Glasgow

MacDonald A, Speirs DC, Greenstreet SPR, Heath MR (2018) Exploring the Influence of Food and Temperature on North Sea Sandeels Using a New Dynamic Energy Budget Model. Front Mar Sci 5:339.

Macer CT (1966) Sand eels (Ammodytidae) in the south-western North Sea; their biology and fishery.

Maniszewska K (2019) Black-legged kittiwake (*Rissa tridactyla*) synchronic delay in laying phenology distribution, its effect on reproductive performance, and relationships with changing environmental conditions. MRes, University of Glasgow

Martins IS, Schrodt F, Blowes SA, Bates AE, Bjorkman AD, Brambilla V, Carvajal-Quintero J, Chow CFY, Daskalova GN, Edwards K, Eisenhauer N, Field R, Fontrodona-Eslava A, Henn JJ, Van Klink R, Madin JS, Magurran AE, McWilliam M, Moyes F, Pugh B, Sagouis A, Trindade-Santos I, McGill BJ, Chase JM, Dornelas M (2023) Widespread shifts in body size within populations and assemblages. Science 381:1067–1071.

Menu C, Pecquerie L, Bacher C, Doray M, Hattab T, Van Der Kooij J, Huret M (2023) Testing the bottom-up hypothesis for the decline in size of anchovy and sardine across European waters through a bioenergetic modeling approach. Prog Oceanogr 210:102943.

Ohlberger J (2013) Climate warming and ectotherm body size - from individual physiology to community ecology. Funct Ecol 27:991–1001.

831 Ohlberger J, Cline TJ, Schindler DE, Lewis B (2023) Declines in body size of sockeye salmon
832 associated with increased competition in the ocean. Proc R Soc B Biol Sci 290:20222248.
833 Ohlberger J, Schindler DE, Ward EJ, Walsworth TE, Essington TE (2019) Resurgence of an
834 apex marine predator and the decline in prey body size. Proc Natl Acad Sci 116:26682–
835 26689.
836 Olin AB (2020) Spatio-temporal variation in lesser sandeel growth and demography: causes and
837 consequences. PhD, University of Strathclyde, Glasgow
838 Olin AB, Banas N, Wright P, Heath M, Nager R (2020) Spatial synchrony of breeding success in
839 the blacklegged kittiwake *Rissa tridactyla* reflects the spatial dynamics of its sandeel
840 prey. Mar Ecol Prog Ser 638:177–190.
841 Olin AB, Banas NS, Johns DG, Heath MR, Wright PJ, Nager RG (2022) Spatio-temporal
842 variation in the zooplankton prey of lesser sandeels: species and community trait patterns
843 from the Continuous Plankton Recorder. ICES J Mar Sci 79:1649–1661.
844 Österblom H, Bignert A, Fransson T, Olsson O (2001) A decrease in fledging body mass in
845 common guillemot *Uria aalge* chicks in the Baltic Sea. Mar Ecol Prog Ser 224:305–309.
846 Persson L, van Leeuwen A, De Roos AM (2014) The ecological foundation for ecosystem-based
847 management of fisheries: mechanistic linkages between the individual-, population-, and
848 community-level dynamics. ICES J Mar Sci 71:2268–2280.
849 Pitcher TJ, Wyche CJ (1983) Predator-avoidance behaviours of sand-eel schools: why schools
850 seldom split. In: Noakes DLG, Lindquist DG, Helfman GS, Ward JA (eds) Predators and
851 prey in fishes. Springer, Dordrecht., p 193–204.
852 Poloczanska ES, Brown CJ, Sydeman WJ, Kiessling W, Schoeman DS, Moore PJ, Brander K,
853 Bruno JF, Buckley LB, Burrows MT, Duarte CM, Halpern BS, Holding J, Kappel CV,

O'Connor MI, Pandolfi JM, Parmesan C, Schwing F, Thompson SA, Richardson AJ (2013) Global imprint of climate change on marine life. Nat Clim Change 3:919–925.

Queiros Q, McKenzie DJ, Dutto G, Killen S, Saraux C, Schull Q (2024) Fish shrinking, energy balance and climate change. Sci Total Environ 906:167310.

R Core Team (2018) R: A language and environment for statistical computing.

Régnier T, Gibb FM, Wright PJ (2017) Importance of trophic mismatch in a winter- hatching species: evidence from lesser sandeel. Mar Ecol Prog Ser 567:185–197.

Régnier T, Gibb FM, Wright PJ (2019) Understanding temperature effects on recruitment in the context of trophic mismatch. Sci Rep 9:15179.

Régnier T, Wright P, Harris M, Gibb F, Newell M, Eerkes-Medrano D, Daunt F, Wanless S (2024) Effect of timing and abundance of lesser sandeel on the breeding success of a North Sea seabird community. Mar Ecol Prog Ser 727:1–17.

Rindorf A, Wright PJ, Jensen H, Maar M (2016) Spatial differences in growth of lesser sandeel in the North Sea. J Exp Mar Biol Ecol 479:9–19.

Robards MD, Anthony JA, Rose GA, Piatt JF (1999) Changes in proximate composition and somatic energy content for Pacific sand lance (*Ammodytes hexapterus*) from Kachemak Bay, Alaska relative to maturity and season. J Exp Mar Biol Ecol 242:245–258.

Robards MD, Rose GA, Piatt JF (2002) Growth and Abundance of Pacific Sand Lance, *Ammodytes hexapterus*, under differing Oceanographic Regimes. Environ Biol Fishes 64:429–441.

Schmidt K, Birchill AJ, Atkinson A, Brewin RJW, Clark JR, Hickman AE, Johns DG, Lohan MC, Milne A, Pardo S, Polimene L, Smyth TJ, Tarran GA, Widdicombe CE, Woodward EMS, Ussher SJ (2020) Increasing picocyanobacteria success in shelf waters contributes

877 to long-term food web degradation. Glob Change Biol 26:5574–5587.
878 Sekiguchi H, Nagoshi M, Horiuchi K, Nakanishi N (1976) Feeding, fat deposits and growth of
879 sand-eels in Ise bay, central Japan. Bull Jpn Soc Sci Fish 42:831–835.
880 Sheridan JA, Bickford D (2011) Shrinking body size as an ecological response to climate
881 change. Nat Clim Change 1:401–406.
882 Swain DP, Sinclair AF, Mark Hanson J (2007) Evolutionary response to size-selective mortality
883 in an exploited fish population. Proc R Soc B Biol Sci 274:1015–1022.
884 Teplitsky C, Millien V (2014) Climate warming and Bergmann's rule through time: is there any
885 evidence? Evol Appl 7:156–168.
886 Tien NSH, Craeymeersch J, Van Damme C, Couperus AS, Adema J, Tulp I (2017) Burrow
887 distribution of three sandeel species relates to beam trawl fishing, sediment composition
888 and water velocity, in Dutch coastal waters. J Sea Res 127:194–202.
889 Tyldesley E, Banas NS, Diack G, Kennedy R, Gillson J, Johns DG, Bull C (2024) Patterns of
890 declining zooplankton energy in the northeast Atlantic as an indicator for marine survival
891 of Atlantic salmon. ICES J Mar Sci 81:1164–1184.
892 Visser AW, Fiksen Ø (2013) Optimal foraging in marine ecosystem models: selectivity,
893 profitability and switching. Mar Ecol Prog Ser 473:91–101.
894 Wanless S, Harris MP, Newell MA, Speakman JR, Daunt F (2018) Community-wide decline in
895 the occurrence of lesser sandeels *Ammodytes marinus* in seabird chick diets at a North
896 Sea colony. Mar Ecol Prog Ser 600:193–206.
897 Wanless S, Wright PJ, Harris MP, Elston DA (2004) Evidence for decrease in size of lesser
898 sandeels *Ammodytes marinus* in a North Sea aggregation over a 30-yr period. Mar Ecol
899 Prog Ser 279:237–246.

900 Wilson RJ, Heath MR (2019) Increasing turbidity in the North Sea during the 20th century due
901 to changing wave climate. Ocean Sci 15:1615–1625.
902 Winslade P (1974a) Behavioural studies on the lesser sandeel *Ammodytes marinus* (Raitt) I. The
903 effect of food availability on activity and the role of olfaction in food detection. J Fish
904 Biol 6:565–576.
905 Winslade P (1974b) Behavioural studies on the lesser sandeel *Ammodytes marinus* (Raitt) II. The
906 effect of light intensity on activity. J Fish Biol 6:577–586.
907 Wootton HF, Morrongiello JR, Schmitt T, Audzijonyte A (2022). Smaller adult fish size in
908 warmer water is not explained by elevated metabolism. Ecol Lett 25: 1177–1188.
909 Wright PJ, Bailey MC (1996) Timing of hatching in *Ammodytes marinus* from Shetland waters
910 and its significance to early growth and survivorship. Mar Biol 126:143–152.
911 Wright PJ, Christensen A, Régnier T, Rindorf A, Van Deurs M (2019) Integrating the scale of
912 population processes into fisheries management, as illustrated in the sandeel, *Ammodytes*
913 *marinus*. ICES J Mar Sci 76:1453–1463.
914 Wright PJ, Orpwood JE, Boulcott P (2017) Warming delays ovarian development in a capital
915 breeder. Mar Biol 164:80.
916 Wright PJ, Orpwood JE, Scott BE (2017) Impact of rising temperature on reproductive
917 investment in a capital breeder: The lesser sandeel. J Exp Mar Biol Ecol 486:52–8.
918

Figures

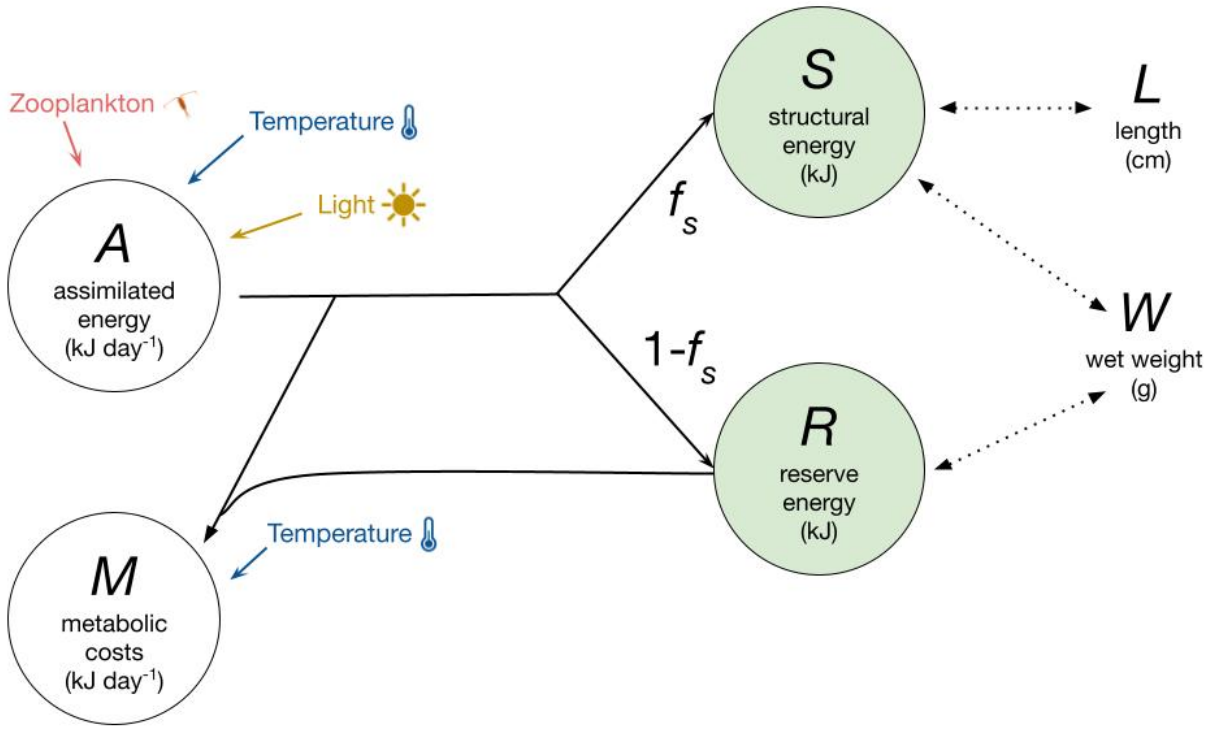

Fig. 1. State variables and key processes in the dynamic energy budget model. Solid black arrows represent energy flows, coloured arrows environmental effects and dotted arrows the relationship between the state variables (S and R) and sandeel length L and wet weight W. f_S is the proportion of net energy gain allocated to structural energy.

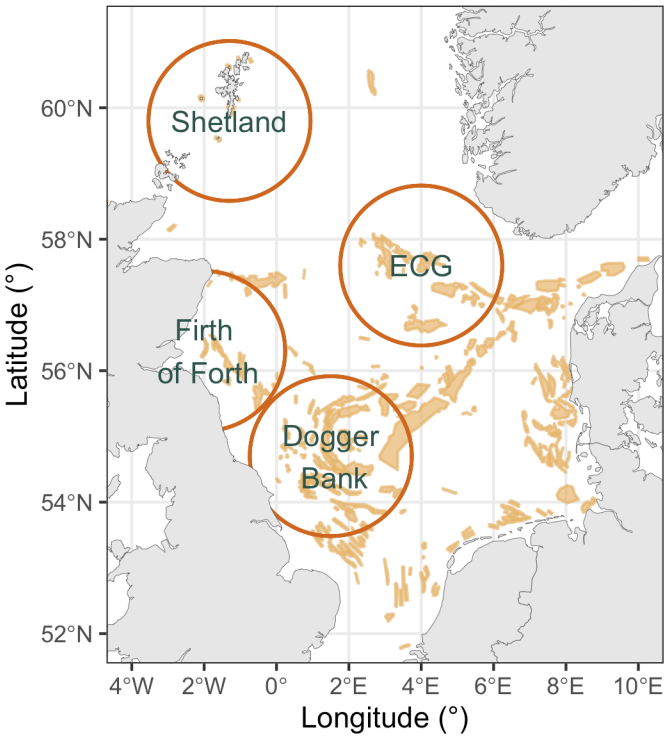

927

928 Fig. 2. Study area, with each location marked with a circle indicating the area from which
929 zooplankton data were sourced (see 2.3). ECG = East Central Grounds. Shaded yellow areas
930 indicate sandeel grounds (Jensen et al. 2011; data from Shetland from Marine Scotland Science).

931

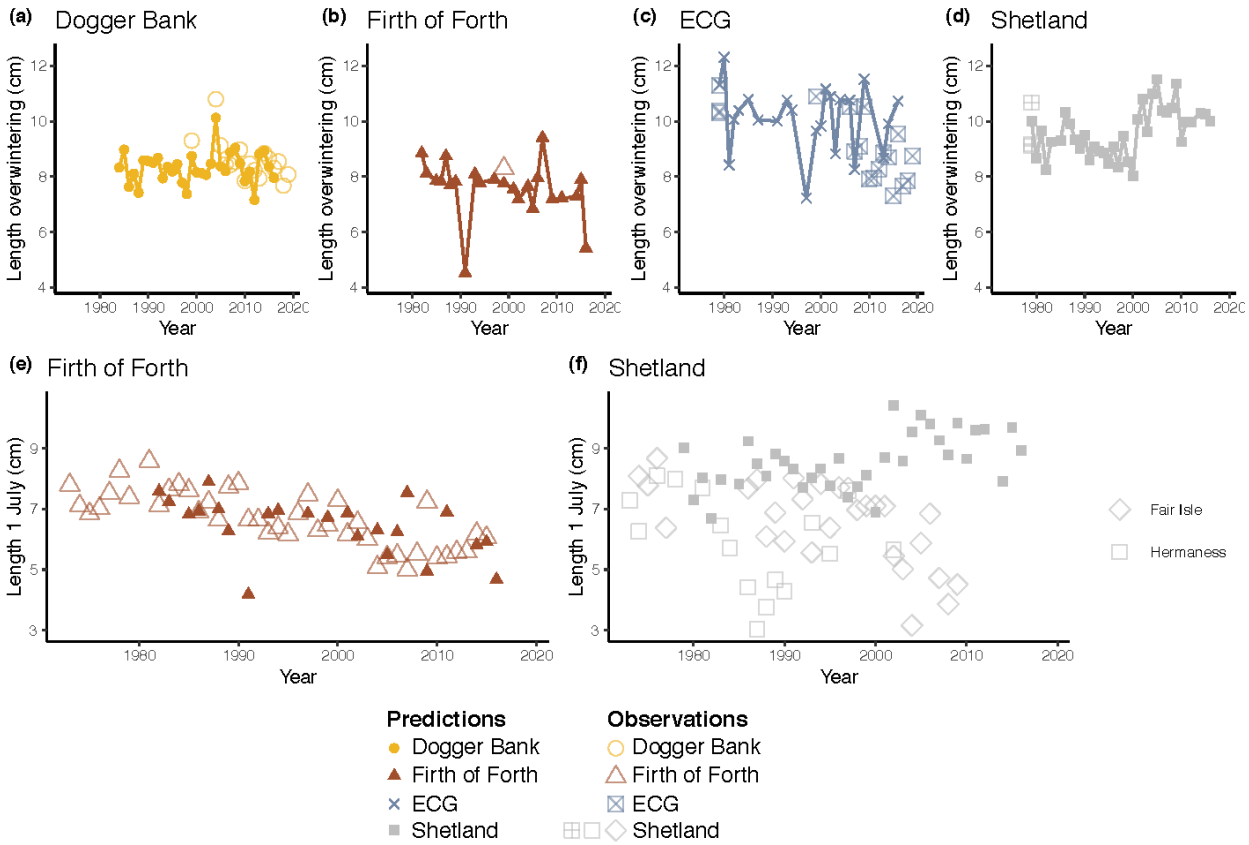

Fig. 3. (a–d) predicted lengths at overwintering for (a) Dogger Bank, (b) Firth of Forth, (c) ECG (East Central Grounds) and (d) Shetland, with corresponding observational data as described in the Methods. (e–f) predicted lengths on the 1st of July for (e) Firth of Forth and (f) Shetland, with corresponding observational data as described in the Methods.

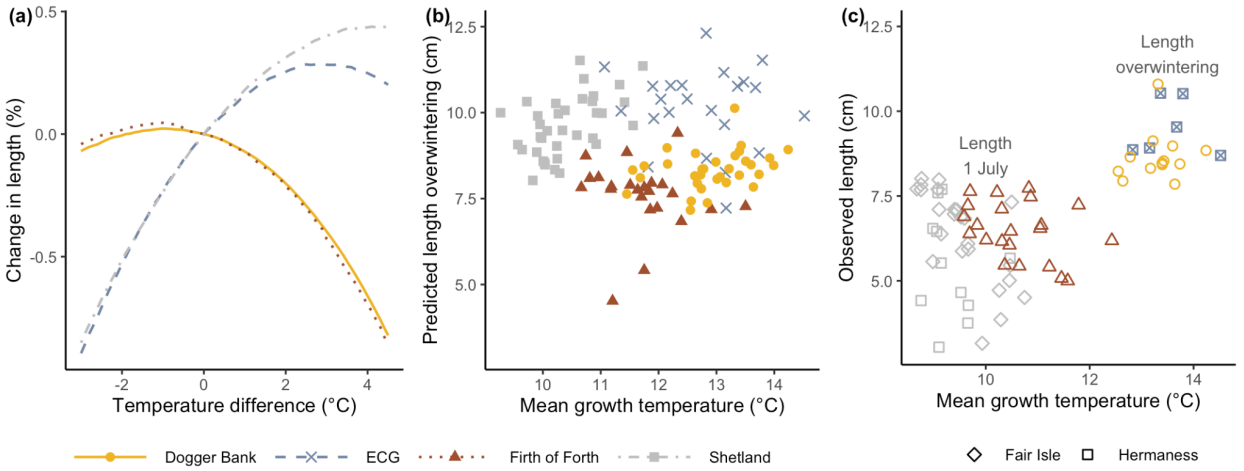

939

940 Fig. 4. Effect of temperature on sandeel length. (a) effect of temperature on predicted lengths at
941 overwintering, in relation to predictions at average temperatures (temperature difference = 0°C).
942 (b) average temperature across the growth season compared to predicted length at overwintering.
943 (c) average temperature from metamorphosis until date of length observations against observed
944 length from field data. Note that for (c), the date of observation varies between locations so that
945 values cannot be compared across locations. Closed symbols are predicted length (b), open
946 symbols observed length (c). ECG = East Central Grounds.

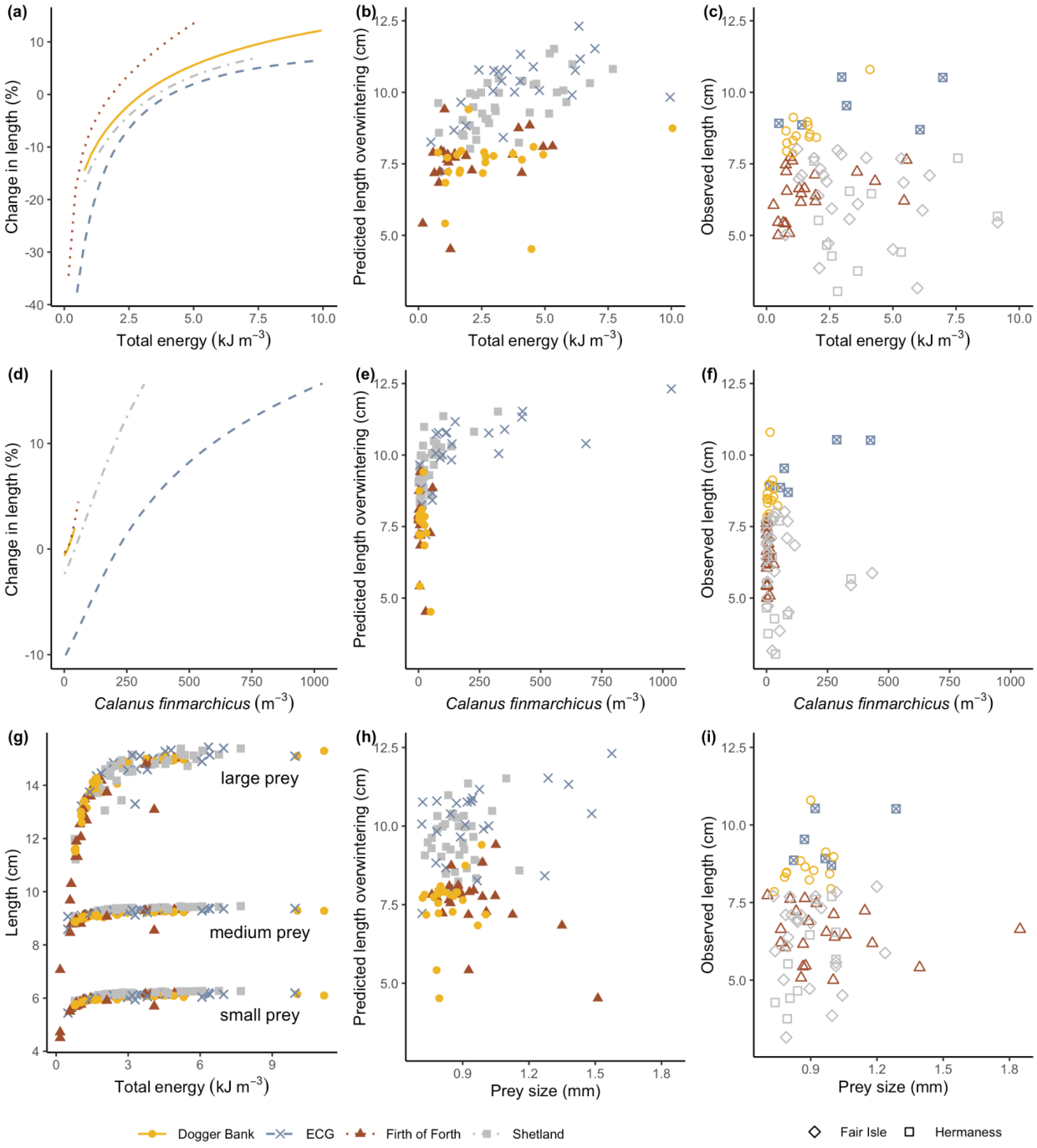

Fig. 5. Effect of food conditions on sandeel growth. (a;d;g) effect of (a) average daily energy availability, (d) density of *Calanus finmarchicus* and (g) prey type on predicted lengths at overwintering. For (a) and (d) length predictions were averaged across years, and predictions are presented in relation to average values. For (g) total available energy for a given day was kept

unchanged, but all energy was provided in the form of large (2.70 mm), medium (1.15 mm), or small (0.16 mm) prey. (b;e;h) predicted length at overwintering compared to (b) average daily energy availability, (e) density of *Calanus finmarchicus* and (h) average prey size across the growth season. (c;f;i) actual length observations from field data compared with (c) average daily energy availability, (f) density of *Calanus finmarchicus* and (i) average prey size across the growth season from metamorphosis until date of length observations. Note that for (c;f;i), the date of observation varies between locations so that values cannot be compared across locations. Closed symbols are predicted length (b;e;h) and open symbols observed length (c;f;i).

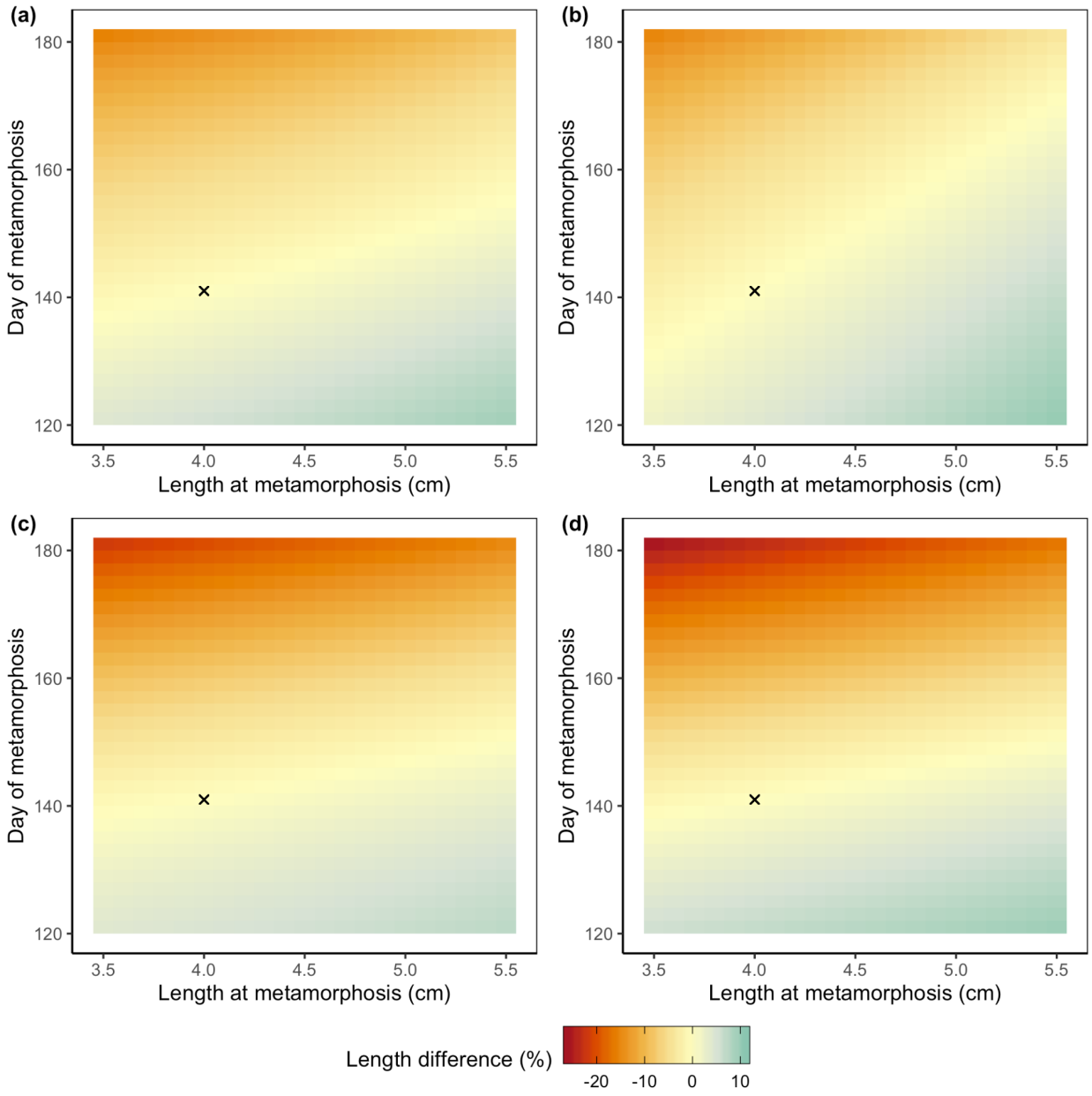

962

963 Fig. 6. Effect of size at metamorphosis and timing of metamorphosis on predicted lengths at

964 overwintering, in relation to predictions for nominal values (marked with x) for (a) Dogger Bank,

965 (b) Firth of Forth, (c) ECG (East Central Grounds) and (d) Shetland.

966

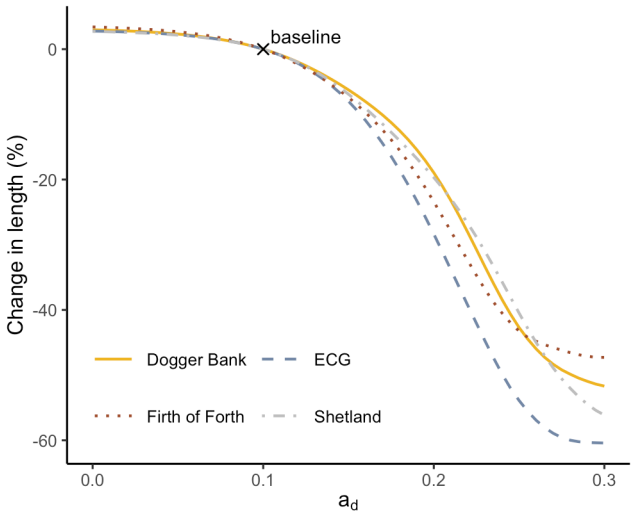

967

968

969 Fig. 7. Effect of turbidity on predicted lengths at overwintering, in relation to predictions for the

970 nominal value (a_d = 0.1). ECG = East Central Grounds.

971